

Computational design of ratiometric two-photon fluorescent Zn^{2+} probes based on quinoline and di-2-picolylamine moieties

Zhe Shao(邵哲), Wen-Ying Zhang(张纹莹), and Ke Zhao(赵珂)

Citation: Chin. Phys. B, 2022, 31 (**5**): 053302. DOI: 10.1088/1674-1056/ac46c6
Journal homepage: http://cpb.iphy.ac.cn; http://iopscience.iop.org/cpb

What follows is a list of articles you may be interested in

Responsive mechanism and coordination mode effect of a bipyridine-based two-photon fluorescent probe for zinc ion

Han Zhang(张瀚), Zhe Shao(邵哲), Ke Zhao(赵珂)
Chin. Phys. B, 2020, 29 (**8**): 083304. DOI: 10.1088/1674-1056/aba9b9

Isomerism and coordination mode effects on two-photon absorption of tris(picolyl)amine-based fluorescent probes for zinc ions

Ke Zhao(赵珂), Jun Song(宋军), Mei-Yu Zhu(朱美玉), Han Zhang(张瀚), Chuan-Kui Wang(王传奎)
Chin. Phys. B, 2018, 27 (**10**): 103301. DOI: 10.1088/1674-1056/27/10/103301

Responsive mechanism and molecular design of di-2-picolylamine-based two-photon fluorescent probes for zinc ions

Mei-Yu Zhu(朱美玉), Ke Zhao(赵珂), Jun Song(宋军), Chuan-Kui Wang(王传奎)
Chin. Phys. B, 2018, 27 (**2**): 023302. DOI: 10.1088/1674-1056/27/2/023302

Responsive mechanism of 2-(2'-hydroxyphenyl)benzoxazole-based two-photon fluorescent probes for zinc and hydroxide ions

Zhang Yu-Jin, Zhang Qiu-Yue, Ding Hong-Juan, Song Xiu-Neng, Wang Chuan-Kui
Chin. Phys. B, 2015, 24 (**2**): 023301. DOI: 10.1088/1674-1056/24/2/023301

Computational design of ratiometric two-photon fluorescent Zn^{2+} probes based on quinoline and di-2-picolylamine moieties

Zhe Shao(邵哲), Wen-Ying Zhang(张纹莹), and Ke Zhao(赵珂)†

School of Physics and Electronics, Shandong Normal University, Jinan 250358, *China*

(Received 3 September 2021; revised manuscript received 17 December 2021; accepted manuscript online 29 December 2021)

To improve two-photon absorption (TPA) response of a newly synthesized probe, a series of ratiometric two-photon fluorescent Zn^{2+} sensors based on quinoline and DPA moieties have been designed. The one-photon absorption, TPA, and emission properties of the experimental and designed probes before and after coordination with Zn^{2+} are investigated employing the density functional theory in combination with response functions. The design consists of two levels. In the first level of design, five probes are constructed through using several electron acceptors or donors to increase accepting or donating ability of the fluorophores. It shows that all the designed probes have stronger TPA intensities at longer wavelengths with respect to the experimental probe because of the increased intra-molecular charge transfer. Moreover, it is found that the probe 4 built by adding an acyl unit has the largest TPA cross section among the designed structures due to the form of longer conjugated length and more linear backbone. One dimethylamino terminal attached along the skeleton can improve TPA intensity more efficiently than two side amino groups. Therefore, in the second level of design, a new probe 7 is formed by both an acyl unit and a dimethylamino terminal. It exhibits that the TPA cross sections of probe 7 and its zinc complex increase dramatically. Furthermore, the fluorescence quantum yields of the designed probes 4 and 7 are calculated in a new way, which makes use of the relation between the computed difference of dipole moment and the measured fluorescence quantum yield. The result shows that our design also improves the fluorescence quantum yield considerably. All in all, the designed probes 4 and 7 not only possess enhanced TPA intensities but also have large differences of emission wavelength upon Zn^{2+} coordination and strong fluorescence intensity, which demonstrates that they are potential ratiometric two-photon fluorescent probes.

Keywords: two-photon absorption, fluorescent probe, zinc ion, intra-molecular charge transfer

PACS: 33.20.–t, 42.65.–k, 82.30.Fi **DOI:** 10.1088/1674-1056/ac46c6

1. Introduction

Two-photon absorption (TPA) active molecules can be used as fluorophores to form fluorescent probes which have important applications in two-photon microscopy (TPM).[1] In comparison with one-photon microscopy, TPM has several advantageous features including higher spatial resolution, deeper penetration depth, lower tissue autofluorescence and self-absorption, less photobleaching and photodamage, and longer observation time.[2–4] Nowadays, great efforts have been exerted for the design and synthesis of two-photon (TP) fluorescent probes with desirable sensing properties for diverse analytes[5–12] based on various recognition mechanisms, such as photon-induced electron transfer (PET), intra-molecular charge transfer (ICT), fluorescent resonance energy transfer, aggregation-induced emission, and so on.[13–16]

Zinc ion is an essential component in enzymes and proteins and involves in many biological processes.[17,18] As such, it is highly required to develop effective fluorescent probes for detecting zinc ions in living system. In recent years, a lot of turn-on or ratiometric TP fluorescent probes for zinc ions have been synthesized based on PET or ICT mechanisms.[5,6] Superior to turn-on probes, ratiometric probes can provide quantitative detection of the analyte by measuring the ratio of emissions at two different wavelengths.[6] Therefore, there is a strong need for the development of ratiometric TP zinc ion probes.

Theoretical study could reveal the structure-property relationships and provide guidelines for the design of functional materials with improving properties.[19–26] At the same computational level, the optical properties of different compounds can be compared accurately. However, contrast to great experimental works, the theoretical study of TP zinc ion probes is still very limited.[27–33] Ren and co-workers[27] designed a series of Salen-based TP zinc ion probes based on ICT mechanism. The one-photon absorption (OPA), TPA and fluorescence emission properties were studied by the quantum chemical calculations. They also performed a theoretical investigation on bipyridine-centered ratiomatric zinc ion probes.[28] Zhang *et al.*[29] elucidated the response mechanisms for a series of 2-(2'-hydroxyphenyl) benzoxazole-containing zinc ion probes by means of response theory. Employing the same computational methods, they also studied a series of TP fluorescent probes for mercury ions.[30] Their work indicated that response functions and density functional theory (DFT) can successfully be used to analyze metal ion probes. In our previ-

†Corresponding author. E-mail: zhaoke@sdnu.edu.cn

© 2022 Chinese Physical Society and IOP Publishing Ltd

ous work,[31] response theory was used to investigate OPA, TPA as well as emission properties of a series of zinc ion probes. Special interests focused on the coordination mode effects.[32,33]

Recently, Li *et al.* synthesized a new ICT-based TP probe for ratiometric imaging and biosensing of Zn^{2+} in living cells.[34] The developed probe has good water solubility and excellent sensitivity and selectivity for ratiometric determining of Zn^{2+}. However, the maximum TPA cross section values were a little lower than the previously reported probes.[34] To improve TPA properties, in this work, we designed a series of ratiometric TP Zn^{2+} probes based on the newly synthesized probe according to ICT mechanism. In the first design, several acceptors or donors were employed to increase the electron accepting or donating ability, accompanying by the change of conjugated length and the dimensionality of charge transfer channel. The OPA and TPA properties of the experimental and designed probes before and after combination with Zn^{2+} were computed at DFT level. The structure-property relationships were analyzed. Then, we performed a second design by picking out the most efficient acceptor and donor from the first design. The TPA property of the second designed probe was calculated and compared with experimental system. At last, the fluorescence properties of the designed probes were computed and evaluated for ratiometric detection. The aim of the design is to achieve the TP probes having not only the large TPA cross section but also strong fluorescence intensity with the significant shift in emission spectrum upon Zn^{2+} coordination. Our research will provide useful guidelines for the design and synthesis of ratiometric TP probes for metal ions.

2. Computational method

In this study, the formulas for calculation of OPA and TPA properties were same as our previous works.[31,32] The 6-31G(d) basis set and the B3LYP hybrid functional were used to optimize the geometries of ground states. On the optimized structures, the OPA properties were computed by the time-dependent DFT (TD-DFT) approach using the same functional and basis set. The geometry optimization of the first excited state and fluorescent emission properties were also calculated using TD-DFT methods at the same level. All the calculations mentioned above were carried out in the Gaussian 16 program.[35] The TPA cross sections were computed by response theory using the B3LYP functional with 6-31G(d) basis set in the Dalton 2013 package.[36] In addition, the effect of methanol solvent is considered by means of the polarizable continuum model in both Gaussian and Dalton calculations. Our previous work has shown that the B3LYP functional calculations can give reasonable TPA properties which are consistent with the trend of experimental observations.[24–26,31,32]

3. Results and discussion

3.1. First design and geometry optimization

The chemical structure of the model probe 1 is depicted in Fig. 1. Probe 1 uses the 1-(pyridin-2-yl)-N-(pyridin-2-ylmethyl)-N-(quinolin-2-ylmethyl)methanamine moiety as Zn^{2+} chelator. The quinoline unit can act both as an electron acceptor of the fluorophore and as a recognition site for Zn^{2+}. The four nitrogen atoms from the quinoline and di-2-picolylamine (DPA) could coordinate with Zn^{2+} by donating lone electron pairs into empty metal orbitals. Because the Zn^{2+}, which has electron withdrawing ability, can connect with the acceptor quinoline group, the ICT from electron donor to acceptor will enhance upon binding with Zn^{2+}, thus improving the TPA intensity as the experiment observed.

To enhance the TPA intensity, one needs to consider the existing structure and TPA property relations. It has been revealed that some structural factors, such as the electron richness and planarity of the π-conjugation center, the molecular symmetry, the strength of donor and acceptor, as well as the conjugated length and dimensionality, have important effects on TPA property.[19–21] On the basis of the model probe, at first, we designed three new structures 2, 3, and 4 by increasing the strength of acceptor, as shown in Fig. 1. It is well known that triazine or diazine group has strong electron-accepting ability and has been often used as the center of multibranched TPA active chromophores.[37] Hence, the quinoline unit is replaced by quinazoline in probe 2 to increase the electron-accepting ability. In probe 3, a cyano group, which is a common acceptor, is added to the quinoline group to increase the acceptor strength. The following acceptor which comes into our mind is the acyl moiety. It is a very flexible acceptor and can also get involved in the Zn^{2+} coordination together with DPA.[38] In our previous work,[31] we have found that the receptor containing acyl and DPA moieties can give rise to higher TPA cross section than the one consisting of pyridine and DPA. As such, an acyl unit is inserted between quinoline and DPA in probe 4. The introduction of acyl moiety can not only strengthen the acceptor, but also extend the conjugated length, which would like to improve TPA response. Then, based on probe 1, we designed another two probes 5 and 6 by increasing the electron-donating ability. The chemical formulas are also presented in Fig. 1. In probe 5, two methyl terminals are substituted by two amino groups, while, in probe 6, the methoxy terminal is replaced by a dimethylamino group because the dimethylamino has stronger ability to donate and transport electrons. Although only one or two functional groups are changed or added in these designed structures to enhance the acceptor or donor strength, the charge transfer dimension, the conjugated length, and the type of coordination bond could also be changed at the same time. Therefore, it would be very interesting to compare the structures and TPA

properties of these probes and find which design way is the most effective one to enhance TPA.

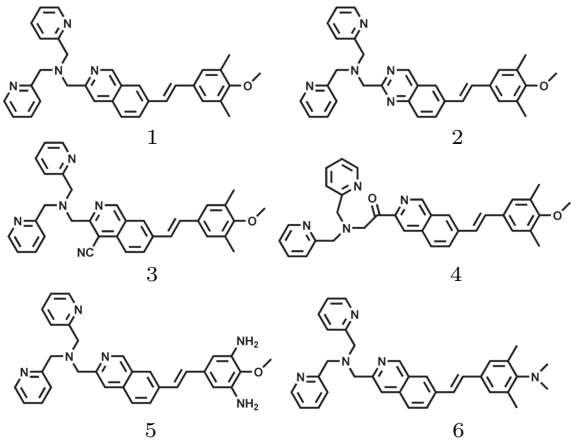


Fig. 1. Chemical structures of the probe 1 and designed probes 2–6.

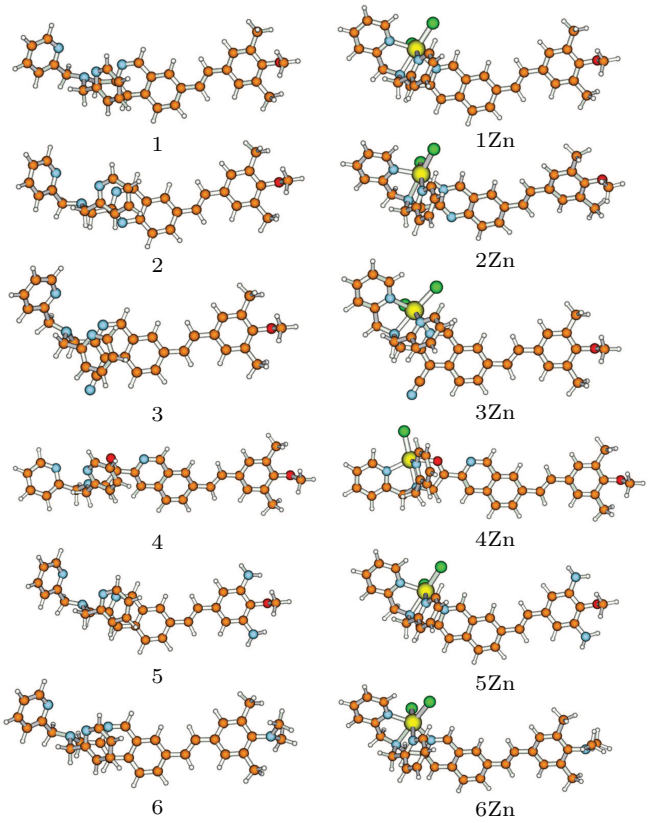


Fig. 2. Optimized geometries of probes 1–6, and the corresponding zinc complexes.

The optimized geometries of these six probes and their zinc complexes are given in Fig. 2. The frequency calculations for all the geometries do not produce any imaginary frequencies. Two Cl^- ions are included explicitly to consider the counter ion effects.[31,39] It is noticed that all the backbones of fluorophore have good planarity. Four coordination bonds can be formed in all the zinc complexes. The Zn^{2+} can chelate both the DPA receptor and the acyl moiety in 4Zn complex. The coordination bond length has the typical value of 2.1 Å–2.3 Å, which is similar to the x-ray crystal data.[38] The structures of 3 and 3Zn are bended a lot due to the steric effect of cyano group. While in 4 and 4Zn, the added acyl moiety leads to a more linear backbone. It should be mentioned that the introduction of the cyano group could affect the binding sites of Zn^{2+} ions for 3Zn. The Zn^{2+} ions could coordinate with the nitrogen atom of the cyano group. We also optimized 3Zn using different initial conformations, but the convergent geometry in which the zinc ion coordinates with both the DPA receptor and the cyano group was not obtained.

The calculated permanent dipole moments and dihedral angles for these structures are presented in Table 1. It shows that the permanent dipole moments of zinc complexes are much larger than those of free ligands. The values of 4 and 4Zn are the largest ones among both free ligands and zinc complexes. The planarity of the backbone can be described by the dihedral angle of two phenyl rings ϕ. It is noticed that most of the structures have nearly planar backbones and the ϕ changes from about 165° to 180°. The ϕ of 6 and 6Zn are equal to 166.13° and 178.47°, respectively. The difference is a little larger than other probes upon binding with zinc ion.

Table 1. Values of permanent dipole moment μ and dihedral angle ϕ.

	μ (D)	ϕ (°)		μ (D)	ϕ (°)
1	6.50	178.14	1Zn	20.41	179.38
2	6.17	172.46	2Zn	18.80	170.03
3	5.18	176.83	3Zn	17.52	176.41
4	11.17	174.89	4Zn	25.50	178.70
5	6.14	178.38	5Zn	18.02	170.75
6	5.81	166.13	6Zn	18.37	178.47

3.2. One-photon absorption

The experimental UV-vis absorption maximum of probe 1 appeared at 360 nm with a broad band. With addition of Zn^{2+}, the absorption increased at 430 nm.[34] Our calculated OPA wavelength λ_{op} and oscillator strength f_{op} of all the studied molecules are listed in Table 2. One can see that λ_{op} of probe 1 is located at the first excited state S_1 with 373 nm, which is close to the value of experiment. The third excited state S_3 also has considerable f_{op}. This means there is another absorption peak at 333 nm with lower intensity. When the molecule binds to Zn^{2+}, both the first and second excited states have strong absorption. The two absorption bands are red-shifted in comparison with the free ligand. This is consistent with the experimental observations. With respect to probe 1, the λ_{op} of the S_1 for all the designed probes is red-shifted significantly because of the stronger acceptor or donor. The values of 3, 4, and 6 come to above 400 nm, which indicates the fluorophores in these molecules are more beneficial to charge transfer. It should be mentioned that the TP probe that can be excited at longer wavelength can increase penetration depth and lower tissue autofluorescence and photobleaching.[3] From Table 2, one can notice that upon Zn^{2+} binding, λ_{op} of the S_1 has a large red-shift for all the designed probes. The red-shift of

4Zn is the largest one and comes to 40 nm. All the structures have more than one absorption bands with different intensities except 4 and its zinc complex 4Zn. In 4 and 4Zn, only the S_1 state has a very strong f_{op}. This is because 4 and 4Zn have good linear skeletons.

Table 2. One-photon absorption properties of the molecules in methanol solvent.

	State	λ_{op} (nm)	f_{op}		State	λ_{op} (nm)	f_{op}
1	S_1	373	0.93	1Zn	S_1	390	0.54
	S_2	339	0.03		S_2	348	0.84
	S_3	333	0.39		S_3	312	0.02
2	S_1	390	0.61	2Zn	S_1	419	0.36
	S_2	362	< 0.01		S_2	349	0.97
	S_3	335	0.80		S_3	336	0.01
3	S_1	413	0.37	3Zn	S_1	447	0.26
	S_2	386	< 0.01		S_2	357	1.01
	S_3	344	1.03		S_3	353	< 0.01
4	S_1	402	1.15	4Zn	S_1	442	1.17
	S_2	383	0.01		S_2	360	< 0.01
	S_3	343	0.02		S_3	353	0.02
5	S_1	391	0.26	5Zn	S_1	413	0.13
	S_2	386	0.52		S_2	407	0.33
	S_3	340	0.34		S_3	361	0.58
6	S_1	403	0.74	6Zn	S_1	426	0.52
	S_2	348	0.05		S_2	375	0.26
	S_3	339	0.57		S_3	349	0.43

The energy gaps between the highest occupied molecular orbital (HOMO) and the lowest unoccupied molecular orbital (LUMO) of these molecules are calculated and the results are illustrated in Fig. 3. One can see that the energy gaps for all the designed probes are lower than the probe 1. Moreover, the values decrease as the zinc complexes are formed. For example, when the probe 4 combines with Zn^{2+}, the energy gap decreases significantly, from 3.40 eV to 3.10 eV. The relatively smaller energy gaps of the zinc complexes compared with corresponding free ligands lead to the red shift of the OPA. 4Zn has the greatest decrease in energy gap, and thereby its red shift is the largest one among zinc complexes. These results indicate that the ICT increases in the designed probes and the OPA process takes place more easily upon binding with Zn^{2+}.

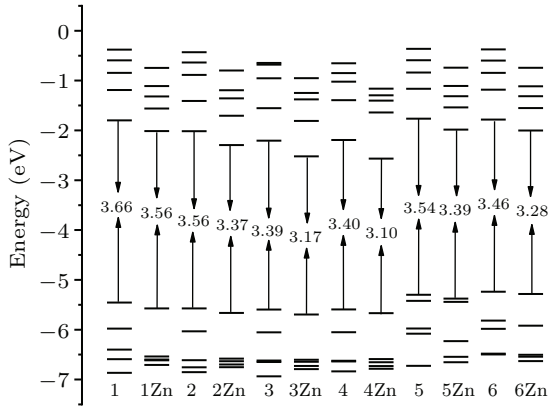


Fig. 3. Frontier orbital energy levels.

3.3. Two-photon absorption

The TPA wavelength λ_{tp} and cross section σ for all the studied molecules in methanol solvent have been calculated by the response theory in Dalton program. The TPA properties of the three lowest excited states are presented in Table 3. For probe 1, the first excited state S_1 has the largest σ, which is equal to 46.0 GM (1 GM = 10^{-50} cm^4·s/photo) at 738 nm. Besides the S_1, the third excited state S_3 also has comparable cross section. When the probe coordinates with Zn^{2+}, the λ_{tp} of S_1 shifts to 778 nm and the corresponding σ increases up to 106.0 GM. The σ of S_2 is much smaller than that of S_1. In experiment, the peak of TPA spectrum is red-shifted from about 720 nm to 750 nm and the cross section is increased from 115 GM to 188 GM after the probe was chelated with Zn^{2+}.[34] Therefore, our TPA calculations agree well with the trend of experiment.

Table 3. Two-photon absorption wavelengths λ_{tp} and cross sections σ of the three lowest excited states of the molecules in methanol solvent.

	State	λ_{tp} (nm)	σ (GM)		State	λ_{tp} (nm)	σ (GM)
1	S_1	738	46.0	1Zn	S_1	778	106.0
	S_2	697	14.0		S_2	697	35.9
	S_3	663	28.9		S_3	663	14.4
2	S_1	770	92.9	2Zn	S_1	838	148.0
	S_2	747	51.5		S_2	719	10.5
	S_3	670	0.9		S_3	705	22.8
3	S_1	819	99.6	3Zn	S_1	899	185.1
	S_2	795	72.3		S_2	766	8.3
	S_3	681	6.5		S_3	745	7.4
4	S_1	795	360.8	4Zn	S_1	883	844.6
	S_2	783	39.2		S_2	778	4.6
	S_3	701	0.17		S_3	749	93.4
5	S_1	780	27.1	5Zn	S_1	841	21.3
	S_2	768	137.5		S_2	824	184.7
	S_3	691	20.6		S_3	730	105.3
6	S_1	790	252.7	6Zn	S_1	847	331.8
	S_2	695	33.3		S_2	747	100.4
	S_3	685	10.3		S_3	695	47.3

For the designed probes 2 and 3, both S_1 and S_2 have comparable TPA intensities. The largest σ of 2 and 3 are 92.9 GM at 770 nm and 99.6 GM at 819 nm, respectively. The λ_{tp} is red-shifted greatly and the σ has about two-fold increase with respect to probe 1. These demonstrate that the substitution of quinazoline and the addition of cyano can increase the ICT and result in TPA enhancement as our expectation. Although the λ_{tp} of probe 3 is much longer than that of probe 2, the largest σ is only slightly higher. This is probably because the probe 3 has more bended backbone from the structure point of view. As for linear probe 4, the TPA mainly focuses on the S_1 and the σ rises to 360.8 GM, much higher than that of probe 1. This implies that the addition of acyl unit is a very efficient way to improve TPA intensity. It not only makes the acceptor strength stronger, but also brings about longer conjugated length and more linear ICT channel. Therefore, one can

realize that various structural factors need to be considered simultaneously for designing TP probes. When the two methyl terminals are substituted by two amino groups, probe 5 has a largest σ of 137.5 GM at the S_2, 768 nm. It is known that the selection rules of one-photon and two-photon transitions are different. The transition between two states with opposite parities are allowed in one-photon process, while same parities are necessary for TPA. The state parity is directly related to the structural symmetry. For a typical symmetric charge-transfer molecule, the second excited state S_2 usually is the most active TPA state.[24] In probe 5, because the two amino groups increase the symmetry of the charge transfer channel, the S_2 produces the largest cross section. In comparison with probe 5, probe 6 has a stronger σ of 252.7 GM at 790 nm. This indicates that enhancing the electron-donating ability along the line of backbone can improve TPA intensity more effectively. In a word, all the designed probes give rise to stronger TPA responses at longer wavelengths in comparison with probe 1, which confirms our design strategies.

Upon binding with Zn^{2+}, the largest σ for all the zinc complexes increases significantly and the corresponding λ_{tp} has a great red-shift. The largest σ of 2Zn rises to 148.0 GM at 838 nm, which has a red-shift of 68 nm with respect to free ligand 2. As for 3Zn, the shift of λ_{tp} comes to 80 nm and the σ of the S_1 becomes to 185.1 GM, much larger than that of probe 3. 4Zn has the largest shift of λ_{tp} like the case of OPA. The red-shift reaches up to 88 nm. The much lower excitation energy makes the σ of 4Zn enhanced greatly. The σ grows to 844.6 GM, more than two times of probe 4. It is also about eight times of zinc complex 1Zn. This demonstrates again that the introduction of an acyl unit can improve TPA intensity very effectively. The receptor consisting of acyl and DPA moieties is beneficial for improving TPA upon coordination with Zn^{2+}. In the case of 5Zn, two strong absorption states appear at about 824 nm and 730 nm with the cross sections of 184.7 GM and 105.3 GM, respectively. The S_2 gives the largest cross section, same as the case of probe 5. While in 6Zn, the σ at 847 nm is 331.8 GM, much larger than that of 5Zn. Therefore, the dimethylamino terminal is better for enhancing TPA intensity. It is noticed that the S_3 of 5Zn and the S_2 of 6Zn also have considerable TPA intensities, which means the change of donor results in more than one absorption bands in the zinc complexes.

3.4. Second design

According to the results of the first design, we have found that the addition of the acyl unit is the most efficient way to increase electron accepting ability and the replacement by one dimethylamino terminal is better than the change of two amino groups for improving TPA intensity. Therefore, in the second design, we construct a new structure using both the acyl unit and the dimethylamino terminal to increase acceptor and donor strengths at the same time. The chemical structures and the optimized geometries for the second designed probe 7 and the corresponding zinc complex 7Zn are shown in Fig. 4.

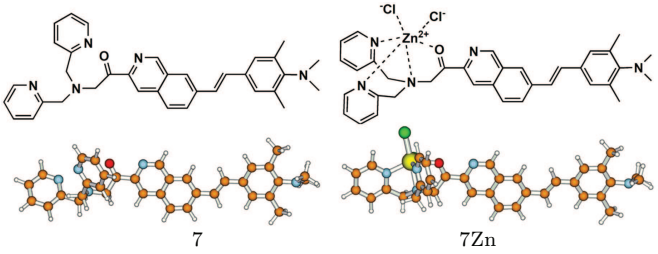


Fig. 4. Chemical structures and optimized geometries of probe 7 and the corresponding zinc complex 7Zn.

As it is expected, the calculated largest σ of 7 and 7Zn rise to 727.8 GM at 874 nm and 1334.2 GM at 997 nm, respectively. The TPA cross section of 7Zn increases one-order of magnitude with respect to 1Zn and the wavelength comes to above 900 nm. As we know, there is a strong need to develop the TP probe that can be excited at longer wavelength ($>$ 900 nm). For a good comparison, the simulated TPA spectra for the probe 1, 4, 7, and their zinc complexes are plotted in Fig. 5. It shows that the spectra of all the structures have one strong TPA peak at different positions. Compared with the experimental probe 1, the absorption intensities of probes 4 and 7 enhance greatly. Upon zinc ion coordination, the absorption wavelength of 4Zn and 7Zn are red-shifted a lot and the absorption intensities are raised about two times with respect to their free ligands. The peak of 7Zn appears at around 1000 nm and the absorption intensity reaches up to 1334.2 GM. Using an acyl unit and a dimethylamino terminal can give rise to a very large increase of TPA cross section due to the enhanced both acceptor and donor strengths.

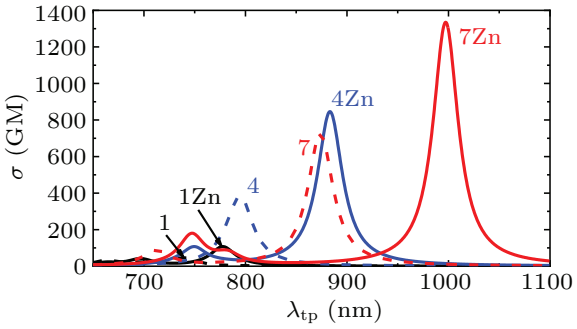


Fig. 5. TPA spectra of probes 1, 4, 7 and the corresponding zinc complexes.

The molecular orbitals that are involved in the strong TPA excitations are also analyzed. The prominent TPA excitation of probes 1 and 7 is the result of the HOMO→LUMO transition. The related orbitals are plotted in Fig. 6. In probe 7, the charge is transferred obviously from the donor dimethylamino terminal to the acceptor acyl moiety. While in probe 1, the charge is transferred very slightly. This indicates that the ICT

of the designed probe 7 is stronger than that of experimental probe 1. Therefore, the designed probe 7 has much higher TPA intensity.[40–42]

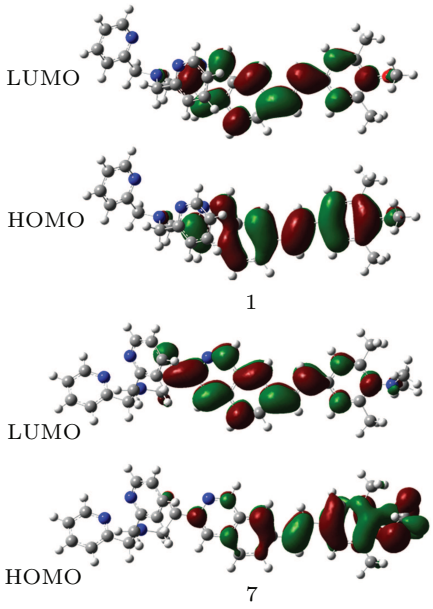


Fig. 6. HOMO and LUMO orbitals of probes 1 and 7.

3.5. Emission property

For ratiometric detection, large difference of emission wavelength between free ligand and zinc complex is necessary. Hence, the emission properties of all the studied molecules have been calculated. The geometry optimization for the first excited state were carried out by the TD-DFT method at B3LYP level with 6-31G(d) basis set in methanol solvent. The obtained fluorescence emission wavelength λ_{em} and corresponding oscillator strength f_{em} are given in Table 4.

Table 4. Values of emission wavelengths λ_{em}, oscillator strengths f_{em}, and the difference of emission wavelengths $\Delta\lambda_{em}$ between the free ligand and the corresponding zinc complex in methanol solvent.

	λ_{em} (nm)	f_{em}		λ_{em} (nm)	f_{em}	$\Delta\lambda_{em}$ (nm)
1	435	1.23	1Zn	470	0.50	35
2	469	0.63	2Zn	542	0.22	73
3	522	0.29	3Zn	590	0.18	68
4	478	1.37	4Zn	546	1.26	68
5	485	0.20	5Zn	531	0.06	46
6	477	1.09	6Zn	522	0.42	45
7	531	1.15	7Zn	634	0.95	103

The λ_{em} of the probe 1 is 435 nm, which tends to the value of experiment, 455 nm. From free ligand to zinc complex, λ_{em} of 1Zn is red-shifted to 470 nm. The difference of emission wavelength $\Delta\lambda_{em}$ is 35 nm. This is consistent with the trend of the experimental data. The oscillator strength f_{em} decreases as the probe 1 coordinates with Zn^{2+}, which indicates that the fluorescent intensity is reduced. It exhibits that $\Delta\lambda_{em}$ of all the designed probes is larger than that of probe 1. For probes 4 and 7, $\Delta\lambda_{em}$ extends to 68 nm and 103 nm, respectively. Moreover, their oscillator strengths are quite high before and after coordination with Zn^{2+}.

An effective TP probe should have significant TPA action cross section, which is the product of the TPA cross section σ and the fluorescence quantum yield ϕ_F. It is essential to optimize both values to develop TP fluorophores for imaging applications. It has been known that the quantum yield has relations to some molecular descriptors. Yamaguchi *et al.*[43] investigated the photophysical properties of conjugated and fused aromatic hydrocarbons and examined correlation between the ϕ_F and magnitude of the π conjugation length in the first excited state.[43] Recently, Humbert-Droz *et al.*[44] performed a high-level calculations for substituted π conjugated terpyridine derivatives and confirmed that the ϕ_F showed a global S-shape dependence on the magnitude of the charge separation, which can be quantified by the change in dipole moments between the ground and excited states. Their work provides a remarkable tool to predict ϕ_F for π conjugated molecules with strong charge transfer character of the first excited state.

Because the compounds studied by Humbert-Droz *et al.*[44] are also linear donor–acceptor-type probes and have similar characters including the molecular elements and sizes to our designed fluorophores, at first, we choose the compounds in their work,[44] together with the model probes 1 and 1Zn, to construct the relation between the measured fluorescence quantum yield and the computed difference of dipole moment. The experimental fluorescence quantum yields of the probe 1 and its zinc complex 1Zn are 0.16 and 0.22, respectively.[34] We calculated their dipole moments of the ground state and the first excited state by TD-DFT method using CAM-B3LYP functional.[44] The lengths of the vector difference of dipole moment $\Delta\mu$ are obtained and the values are 0.7343 e·Å and 1.3176 e·Å. The data of the experimental ϕ_F and the calculated $\Delta\mu$ for probes 1 and 1Zn, and the compounds 1a–1e and 1g, which are taken from Ref. [44], are presented in Fig. 7. Their relation can be fitted by the exponential function as[43,44]

$$\phi_F = \frac{1}{1+\exp(A\Delta\mu + B)}, \tag{1}$$

where A and B are the fitting parameters. To our pleasant surprise, the points of 1 and 1Zn are nearly located on the fitting line, which is almost same as the one obtained by Humbert-Droz *et al.*[44] This demonstrates that the relation is very suitable and reliable for our studied systems. The relation shows the ϕ_F has a nearly linear dependence on $\Delta\mu$ in a certain range.

Then, according to the obtained relation, the $\Delta\mu$ and the ϕ_F are calculated for the designed probes 4 and 7, and their zinc complexes. The results are given in Table 5. The ϕ_F of 1 and 1Zn are also calculated for comparison. It is found that the

ϕ_F of 1 and 1Zn are in a very good agreement with experimental data. The ϕ_F of the probes 4 and 7 increase to a great extent with respect to probe 1. The ϕ_F of probe 7 is about twice as high as the probe 1. The ϕ_F of the zinc complexes 4Zn and 7Zn are both a little larger than those of their free ligands 4 and 7, which is consistent with experimental observations on probe 1.

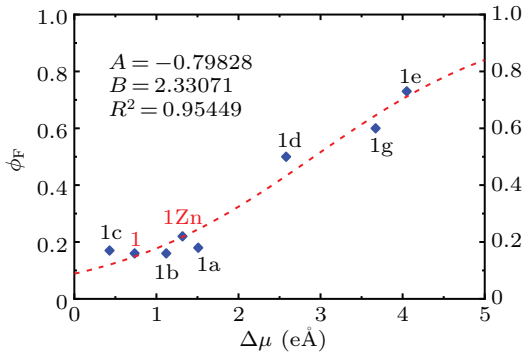


Fig. 7. The experimental fluorescence quantum yield ϕ_F as a function of calculated difference of dipole moment $\Delta\mu$ for probe 1 and its zinc complex 1Zn, and the compounds studied in Ref. [44]. The dotted line corresponds to the fit obtained with Eq. (1). The fitting parameters A and B, and the squared correlation coefficient R^2 are provided.

Finally, TPA and fluorescence properties are considered together and the TPA action cross section $\phi_F\sigma$ are computed (see Table 5). The $\phi_F\sigma$ of the designed probes 4 and 7 are enhanced dramatically, which demonstrates that they have very strong TP excited fluorescent intensity and are expected to have superior performance for imaging applications. Our design not only improves the TPA cross section, but also enhances the fluorescence quantum yield.

Table 5. The lengths of the difference of the dipole moments between the ground state and the first excited states $\Delta\mu$, the fluorescence quantum yields ϕ_F, the TPA cross sections σ, and the TPA action cross sections $\phi_F\sigma$.

	$\Delta\mu$ (eÅ)	ϕ_F	σ (GM)	$\phi_F\sigma$ (GM)
1	0.7343	0.149 (0.16)[a]	46.0	6.8
1Zn	1.3176	0.218 (0.22)[a]	106.0	23.1
4	1.5782	0.255	360.8	92.1
4Zn	2.2851	0.376	844.6	317.6
7	1.9815	0.321	727.8	233.7
7Zn	2.6878	0.454	1334.2	605.5

[a]Experimental value (Li *et al.*[34]).

It should be noticed that all the probes could have various isomers which might produce different fluorescent properties. The effect of isomerism needs to be considered. Starting from different initial configuration, the geometry optimization of probe 1 gives other four equilibrium conformations 1ISa-1ISd, as shown in Fig. 8. In much the same way, four isomers 7ISa–7ISd are also obtained for probe 7 (Fig. 8) It can be seen that these isomers differ by the orientations of pyridines in DPA groups.

The $\Delta\mu$ and the ϕ_F are calculated for the various isomers and the results are listed in Table 6. The various conformations of probe 1 give rise to nearly same ϕ_F, which is very close to the experimental value 0.16. In the case of the designed probe 7, the difference of ϕ_F is also very small (< 0.03). Furthermore, all the ϕ_F are above 0.3, much higher than that of probe 1. This indicates that the isomerism has a trivial effect on the fluorescence quantum yield, and the designed probe is expected to have stronger fluorescent intensity.

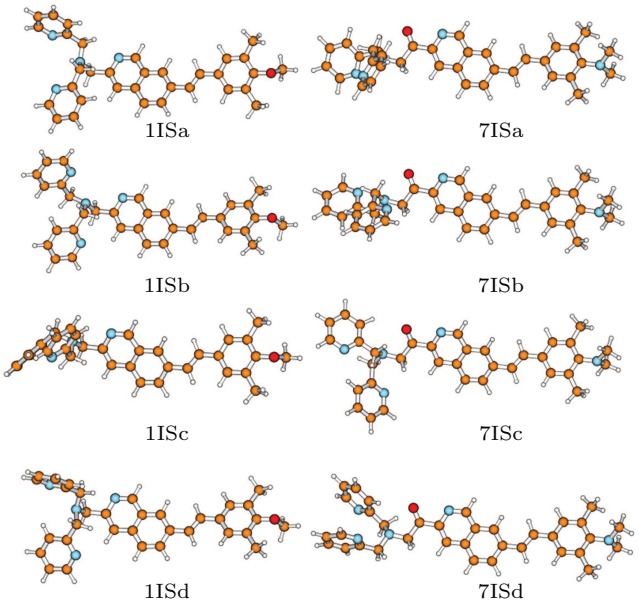


Fig. 8. Optimized geometries of the various isomers for probes 1 and 7.

Table 6. The lengths of the difference of the dipole moments between the ground state and the first excited states $\Delta\mu$ and the fluorescence quantum yields ϕ_F of the various isomers for probes 1 and 7.

	$\Delta\mu$ (e·Å)	ϕ_F		$\Delta\mu$ (e·Å)	ϕ_F
1ISa	0.7318	0.148	7ISa	2.0189	0.328
1ISb	0.6727	0.143	7ISb	1.8955	0.306
1ISc	0.7577	0.151	7ISc	1.9937	0.323
1ISd	0.7285	0.148	7ISd	2.0470	0.333

4. Conclusion

A series of ratiometric TP fluorescent Zn^{2+} sensors containing quinoline and DPA moieties have been designed based on a newly synthesized probe. At first, five structures are designed by using the diazine, cyano and acyl groups to increase acceptor strength and the amino and dimethylamino terminals to enhance electron donating ability. The OPA and TPA properties of the experimental and designed probes before and after combination with Zn^{2+} are computed at a DFT level. The calculated OPA and TPA wavelengths and TPA cross sections are consistent with the experimental trends. It shows that the OPA and TPA wavelengths is red-shifted and the TPA cross section is enhanced greatly because of the increased ICT mechanism upon metal binding. As expected, all the designed probes give rise to strong TPA responses at longer wavelengths. It is interesting to find that the addition of the acyl unit in the designed

probe 4 is the most efficient way to increase TPA cross section due to the form of longer conjugated length and more linear backbone. It also reveals that one dimethylamino terminal attached along the skeleton can improve TPA intensity more efficiently than two side amino groups. Then, based on these results, we performed a second design using the most efficient acyl unit and dimethylamino terminal to increase both acceptor and donor strengths. The calculated TPA cross sections of the second designed probe 7 and its zinc complex 7Zn enhance significantly and the TPA wavelength of 7Zn exceeds 900 nm. At last, the emission properties of all the studied molecules are calculated by optimizing the first excited state. It exhibits that the designed probes 4 and 7 have large differences of emission wavelength between free ligand and zinc complex, which demonstrates that they are suitable for ratiometric detection. The fluorescence quantum yields ϕ_F of the designed probes 4 and 7 have also been calculated using the relation of the computed difference of dipole moment and the experimental ϕ_F. It shows that the ϕ_F of the designed probes increase considerably. Our design is so successful that both the TPA cross section and the quantum yield are improved greatly. This work provides useful guidelines for the design of efficient ratiometric TP probes for zinc ions.

Acknowledgement

Project supported by the Shandong Provincial Natural Science Foundation, China (Grant No. ZR2020MA078).

References

[1] Denk W, Strickler J H and Webb W W 1990 *Science* **248** 73
[2] Yao S and Belfield K D 2012 *Eur. J. Org. Chem.* **2012** 3199
[3] Kim D, Ryu H G and Ahn K H 2014 *Org. Biomol. Chem.* **12** 4550
[4] Kim H M and Cho B R 2015 *Chem. Rev.* **115** 5014
[5] Kim H M and Cho B R 2011 *Chem. Asian J.* **6** 58
[6] Sarkar A R, Kang D E, Kim H M and Cho B R 2014 *Inorg. Chem.* **53** 1794
[7] Sumalekshmy S and Fahrni C J 2011 *Chem. Mater.* **23** 483
[8] Kim D, Singha S, Wang T, Seo E, Lee J H, Lee S J, Kim K H and Ahn K H 2012 *Chem. Commun.* **48** 10243
[9] Kim H J, Heo C H and Kim H M 2013 *J. Am. Chem. Soc.* **135** 17969
[10] Masanta G, Heo C H, Lim C S, Bae S K, Cho B R and Kim H M 2012 *Chem. Commun.* **48** 3518
[11] Kucherak O A, Didier P, Mély Y and Klymchenko A S 2010 *J. Phys. Chem. Lett.* **1** 616
[12] Zhang J, Chai X, He X P, Kim H J, Yoon J and Tian H 2019 *Chem. Soc. Rev.* **48** 683
[13] de Silva A P, Gunaratne H Q N, Gunnlaugsson T, Huxley A J M, McCoy C P, Rademacher J T and Rice T E 1997 *Chem. Rev.* **97** 1515
[14] Sapsford K E, Berti L and Medintz I L 2006 *Angew. Chem. Int. Ed.* **45** 4562
[15] Wu J, Liu W, Ge J, Zhang H and Wang P 2011 *Chem. Soc. Rev.* **40** 3483
[16] Kwok R T K, Leung C W T, Lam J W Y and Tang B Z 2015 *Chem. Soc. Rev.* **44** 4228
[17] Bush A I, Pettingell W H, Multhaup G, Paradis M d, Vonsattel J P, Gusella J F, Beyreuther K, Masters C L and Tanzi R E 1994 *Science* **265** 1464
[18] Bush A I and Tanzi R E 2002 *Proc. Natl. Acad. Sci. USA* **99** 7317
[19] Pawlicki M, Collins H A, Denning R G and Anderson H L 2009 *Angew. Chem. Int. Ed.* **48** 3244
[20] Kim H M and Cho B R 2009 *Chem. Commun.* **0** 153
[21] He G S, Tan L S, Zheng Q D, Prasad P N 2008 *Chem. Rev.* **108** 1245
[22] Mu X, Wang J and Sun M 2019 *J. Phys. Chem. C* **123** 14132
[23] Mu X, Wang X, Quan J and Sun M 2020 *J. Phys. Chem. C* **124** 4968
[24] Zhao K, Ferrighi L, Frediani L, Wang C K and Luo Y 2007 *J. Chem. Phys.* **126** 204509
[25] Zhao K and Luo Y 2010 *J. Phys. Chem. B* **114** 13167
[26] Wang F Q, Zhao K, Zhu M Y and Wang C K 2016 *J. Phys. Chem. B* **120** 9708
[27] Huang S, Zou L Y, Ren A M, Guo J F, Liu X T, Feng J K and Yang B Z 2013 *Inorg. Chem.* **52** 5702
[28] Wang D, Ren A M, Zou L Y, Guo J F and Huang S 2017 *J. Photochem. Photobiol. A Chem.* **341** 20
[29] Zhang Y J, Zhang Q Y, Ding H J, Song X N and Wang C K 2015 *Chin. Phys. B* **24** 023301
[30] Leng J, Xin J, Zhou H, Li K, Hu W and Zhang Y 2021 *Int. J. Quantum Chem.* **121** e26435
[31] Zhu M Y, Zhao K, Song J and Wang C K 2018 *Chin. Phys. B* **27** 023302
[32] Zhao K, Song J, Zhu M Y, Han Z and Wang C K 2018 *Chin. Phys. B* **27** 103301
[33] Zhang H, Shao Z and Zhao K 2020 *Chin. Phys. B* **29** 083304
[34] Li W, Liu Z, Fang B, Jin M and Tian Y 2020 *Biosens. Bioelectron.* **148** 111666
[35] Frisch M J, Trucks G W, Schlegel H B, *et al.* 2016 Gaussian 16, Revision C.01 Gaussian Inc. Wallingford CT
[36] Aidas K, Angeli C, Bak K L, *et al.* 2014 *WIREs Comput. Mol. Sci.* **4** 269
[37] Jiang Y, Wang Y, Wang B, Yang J, He N, Qian S and Hua J 2011 *Chem. Asian J.* **6** 157
[38] Xue L, Fang Z, Li G, Wang H and Jiang H 2011 *Sens. Actuator B-Chem.* **156** 410
[39] Sumalekshmy S, Henary M M, Siegel N, Lawson P V, Wu Y, Schmidt K, Brédas J L, Perry J W and Fahrni C J 2007 *J. Am. Chem. Soc.* **129** 11888
[40] Mu X, Zong H, Zhu L and Sun M 2020 *J. Phys. Chem. C* **124** 2319
[41] Cui L, Zhu S and Sun M 2021 *Physica E* **134** 114840
[42] Cui L, Li R, Mu T, Wang J, Zhang W and Sun M 2022 *Spectrochim. Acta A Mol. Biomol. Spectrosc.* **264** 120283
[43] Yamaguchi Y, Matsubara Y, Ochi T, Wakamiya T and Yoshida Z I 2008 *J. Am. Chem. Soc.* **130** 13867
[44] Humbert-Droz M, Piguet C and Wesolowskic T A 2016 *Phys. Chem. Chem. Phys.* **18** 29387